NASA TECHNICAL NOTE

NASA TN D-6357

NASA TN D-6357

WAVE SURFACES DUE TO IMPACT ON ANISOTROPIC FIBER COMPOSITE PLATES

by Francis C. Moon

Lewis Research Center

Cleveland, Ohio 44135

NATIONAL AERONAUTICS AND SPACE ADMINISTRATION • WASHINGTON, D. C. • SEPTEMBER 1971

1. Report No.	2. Government Accession No.	3. Recipient's Catalog No.
NASA TN D-6357		

4. Title and Subtitle	5. Report Date
WAVE SURFACES DUE TO IMPACT ON ANISOTROPIC FIBER COMPOSITE PLATES	September 1971
	6. Performing Organization Code

7. Author(s)	8. Performing Organization Report No.
Francis C. Moon	E-6150
	10. Work Unit No. 129-03
9. Performing Organization Name and Address Lewis Research Center National Aeronautics and Space Administration Cleveland, Ohio 44135	11. Contract or Grant No.
	13. Type of Report and Period Covered Technical Note
12. Sponsoring Agency Name and Address National Aeronautics and Space Administration Washington, D.C. 20546	14. Sponsoring Agency Code

15. Supplementary Notes

16. Abstract

The application of advanced fiber composite materials to the fabrication of fan or compressor blades depends on their ability to sustain limited damage under impact forces. For small objects such as pebbles or hailstones, the impact times are of the order of microseconds. Thus the energy transmission to the blade is completed before there are any or many reflections from the boundaries. The stress waves induced in anisotropic plates by transverse, short-duration impact forces are examined in this report. The anisotropy is related to the layup angles of the fibers. Using a modification of Mindlin's approximate theory of plates, it is shown that both extensional and bending waves are generated by transverse impact. The magnitudes of the wave velocities in different directions are calculated for graphite fiber-epoxy matrix plates as well as boron-aluminum and glass-epoxy systems for various layup angles. Finally the shapes of the wave fronts or wave surfaces due to point impact are also presented for the cases mentioned.

17. Key Words (Suggested by Author(s))	18. Distribution Statement
Impact Stress waves Composite materials Laminates Composites	Unclassified - unlimited

19. Security Classif. (of this report)	20. Security Classif. (of this page)	21. No. of Pages	22. Price*
Unclassified	Unclassified	25	$3.00

*For sale by the National Technical Information Service, Springfield, Virginia 22151

WAVE SURFACES DUE TO IMPACT ON ANISOTROPIC FIBER COMPOSITE PLATES

by Francis C. Moon*

Lewis Research Center

SUMMARY

The use of advanced fiber composite materials for fabricating fan or compressor blades depends on the ability of the materials to sustain limited damage under impact forces. For foreign objects whose masses are comparable to that of the blade, such as large birds, one can expect impact times of the order of the lower blade vibration periods. For these cases the method of vibrations should prove adequate to the task of predicting the impact stresses and possible failure modes. For smaller objects such as pebbles or hailstones, the impact times are of the order of microseconds. Thus the energy transmission to the blade is completed before there are any or many reflections from the boundaries. It is for this class of problems that a stress wave analysis is more useful than vibratory methods of analysis. The stress waves induced in anisotropic plates by transverse, short-duration impact forces are examined in this report. The anisotropy is related to the layup angles of the fibers, which lie in the plane of the plate. Using a modification of Mindlin's approximate theory of plates, it is shown that both extensional and bending waves are generated by transverse impact. The magnitudes of the wave velocities in different directions are calculated for graphite fiber-epoxy matrix plates as well as boron-aluminum and glass-epoxy systems for various layup angles. Finally, the shapes of the wave fronts or wave surfaces due to point impact are also presented for the cases mentioned.

INTRODUCTION

The successful application of advanced fiber composite materials to jet engine fan or compressor blades will depend in part on the ability of these materials to withstand the

*Assistant Professor of Aerospace and Mechanical Sciences, Princeton University, Princeton, New Jersey; NASA Summer Faculty Fellow in 1970.

forces of impact due to foreign objects. Such impact can be the result of the ingestion of stones, nuts and bolts, hailstones, or birds into a jet engine. The relative velocity of the impacting body to the blade can be in the order of 450 meters per second (1500 ft/sec). The ingestion of objects of sizeable mass (e.g., birds) might involve the dynamics of the entire blade. The high speed impact of small objects will result in small impact times ($<50\ \mu$sec), and the initial transmission of impact energy into a local region of the blade. This initial energy will propagate into the rest of the blade in the form of stress waves. Although such high speed impact will involve local cratering or even complete penetration, long range damage away from the impact area can result from the reflection of stress waves (spalling) and focusing due to changes in geometry.

It is also observed that materials under high rates of strain exhibit an increased tensile strength and decreased ductility. Such evidence tends to validate the use of elastic wave analysis for the determination of the prefracture stresses induced by the impact forces. However, even if plastic waves do predominate, elastic precursor waves will bound the stressed impact zone.

In this report, calculations of velocity and wave surfaces in anisotropic composite plates due to transverse impact forces are presented. These wave surfaces, for a given time after impact, bound the stressed region surrounding the impact point.

REVIEW OF BASIC EQUATIONS OF ANISOTROPIC ELASTIC PLATES

The composite plates under consideration are imagined to comprise a number of unidirectional plys (fig. 1). An equal number of plys lie at angles $\pm\varphi$ from the symmetry axis in such a manner that bending-extensional coupling does not result. We also assume that the number of plys across the plate thickness is reasonably large, so that average properties across the plys can be used. This approximation will be valid for wavelengths greater than the ply thickness and certainly valid for wavelengths greater than the plate thickness.

Thus, in place of the n-ply plate, the wave propagation in an equivalent anisotropic plate is being studied. The equivalent elastic constants are obtained from a static analysis of the n-ply composite plate.

The equations of motion for a linear anisotropic elastic body are (ref. 1)

$$t_{ij,j} = \rho\ddot{u}_i \tag{1}$$

(The double summation convention is assumed, the dots indicate time differentiation, and the notation $\varphi_{,j}$ stands for $\partial\varphi/\partial x_j$ where x_j is a Cartesian coordinate.) The vector u is the displacement, and body forces are assumed to be absent. In general, the stress

tensor t_{ij} is related to the strains $e_{k\ell}$ through the equations (ref. 1)

$$t_{ij} = C_{ijk\ell} e_{k\ell} \tag{2}$$

There are only 21 independent elastic constants $C_{ijk\ell}$ in general. For orthotropic symmetry, which pertains to the composite plates under consideration, the stress-strain equations take the following matrix form:

$$\begin{bmatrix} t_{11} \\ t_{22} \\ t_{33} \\ t_{23} \\ t_{13} \\ t_{12} \end{bmatrix} = \begin{bmatrix} C_{11} & C_{12} & C_{13} & 0 & 0 & 0 \\ C_{12} & C_{22} & C_{23} & 0 & 0 & 0 \\ C_{13} & C_{23} & C_{33} & 0 & 0 & 0 \\ 0 & 0 & 0 & C_{44} & 0 & 0 \\ 0 & 0 & 0 & 0 & C_{55} & 0 \\ 0 & 0 & 0 & 0 & 0 & C_{66} \end{bmatrix} \begin{bmatrix} e_{11} \\ e_{22} \\ e_{33} \\ 2e_{23} \\ 2e_{13} \\ 2e_{12} \end{bmatrix} \tag{3}$$

The constants $C_{\alpha\beta}$ ($\alpha, \beta = 1, 2, \ldots, 6$) are of course related to the $C_{ijk\ell}$. The strains are related to the displacements in the body by

$$e_{ij} = \frac{1}{2}(u_{i,j} + u_{j,i}) \tag{4}$$

Combining equations (1), (2), and (4) results in the following partial differential equations:

$$C_{ijk\ell} u_{k,\ell j} = \rho \ddot{u}_i \tag{5}$$

Wave propagation in anisotropic media has been studied for a long time (refs. 2 and 3); however, very few problems have been solved in which boundaries are present.

The approximate theory of anisotropic plates to be used in this study is due to Mindlin and coworkers (refs. 4 and 5). In their theory the three-dimensional displacement is expanded in Legendre polynomials in the thickness direction.

$$\underline{u} = \sum_{n=0}^{\infty} P_n(\eta) \underline{u}^{(n)}(x_1, x_3, t) \tag{6}$$

where $\eta = x_2/b$ and b is half the plate thickness and where

$$P_0(\eta) = 1$$

$$P_1(\eta) = \eta$$

$$P_2(\eta) = \frac{3\eta^2 - 1}{2}$$

The $\{P_n(\eta)\}$ are orthogonal:

$$\int_{-1}^{1} P_n P_m \, d\eta = \begin{cases} 0 & n \neq m \\ \dfrac{2}{2n+1} & n = m \end{cases}$$

The functions $u^{(n)}$ have a physical significance (see ref. 5, pp. 563-564): u_1^0, u_3^0 represent in-plane or extensional deformation; u_2^0 represents the transverse displacement of the plate; u_1^1 and u_3^1 are measures of the bending strains or $b\psi_1$, $b\psi_2$ where ψ_1 is the slope of the plate midsurface due to bending about the 3-axis; and u_2^1 is a measure of the thickness stretching.

To obtain the approximate equations of motion, a variational method is used (ref. 4). Instead of solving equation (5) directly, the equations are integrated across the thickness:

$$\int_A \int_{-1}^{1} (t_{ij,i} - \rho \ddot{u}_j) \delta u_j b \, d\eta \, dA = 0 \tag{7}$$

where δu_j and t_{ij} are calculated using the series representation of the displacement (eq. (6)). This leads to an infinite set of equations each involving higher modes of vibration of the plate:

$$b t_{\alpha j, \alpha}^{(n)} + \left[P_n(\eta) t_{2j} \right]_{-1}^{1} - t_{2j}^{(n)} = \rho b \, \frac{2}{2\eta + 1} \, \ddot{u}_j^{(n)} \tag{8}$$

where $\alpha = 1, 3$.

$$t_{\alpha j}^{(n)} = \int_{-1}^{1} P_n(\eta) t_{\alpha j}\, d\eta$$

$$t_{2j}^{(n)} = \int_{-1}^{1} \frac{dP_n}{d\eta}\, t_{2j}\, d\eta$$

If impact forces are present on the upper surface of the plate, then the following boundary conditions are used to evaluate the second terms, $\left[P_n(\eta) t_{2j}\right]_{-1}^{1}$ in equation (8).

$$\left.\begin{aligned} t_{22}(\eta = 1) &= q_2 \\ t_{22}(\eta = -1) &= 0 \\ t_{21}(\eta = \pm 1) &= 0 \\ t_{23}(\eta = \pm 1) &= 0 \end{aligned}\right\} \qquad (9)$$

This scheme has been carried out for $n = 0, 1, 2$ for orthogonal symmetry. The equations of motion for u_1^0 and u_3^0 and u_2^0, u_1^1, and u_3^1 are shown in equations (10) and (11), respectively:

$$\left.\begin{aligned} \rho \frac{\partial^2 u_1^0}{\partial t^2} &= C_{11} \frac{\partial^2 u_1^0}{\partial x_1^2} + C_{55} \frac{\partial^2 u_1^0}{\partial x_3^2} + (C_{55} + C_{13}) \frac{\partial^2 u_3^0}{\partial x_1\, \partial x_3} + C_{12} \frac{1}{b} \frac{\partial u_2^1}{\partial x_1} \\ \rho \frac{\partial^2 u_3^0}{\partial t^2} &= C_{33} \frac{\partial^2 u_3^0}{\partial x_3^2} + C_{33} \frac{\partial^2 u_3^0}{\partial x_1^2} + (C_{55} + C_{13}) \frac{\partial^2 u_1^0}{\partial x_1\, \partial x_3} + C_{32} \frac{1}{b} \frac{\partial u_2^1}{\partial x_3} \end{aligned}\right\} \qquad (10)$$

$$\left.\begin{aligned}
\rho \frac{\partial^2 u_2^0}{\partial t^2} &= C_{66} \frac{\partial^2 u_2^0}{\partial x_1^2} + C_{44} \frac{\partial^2 u_2^0}{\partial x_3^2} + C_{66} \frac{1}{b} \frac{\partial u_1^1}{\partial x_1} + C_{44} \frac{1}{b} \frac{\partial u_3^1}{\partial x_3} + \frac{1}{2b} q_2 \\
\rho \frac{\partial^2 u_1^1}{\partial t^2} &= C_{11} \frac{\partial^2 u_1^1}{\partial x_1^2} + C_{55} \frac{\partial^2 u_1^1}{\partial x_3^2} + (C_{55} + C_{13}) \frac{\partial^2 u_3^1}{\partial x_1 \partial x_3} - \frac{3}{b}\left[C_{66}\left(\frac{\partial u_2^0}{\partial x_1} + \frac{u_1^1}{b}\right) - C_{12} \frac{\partial u_2^{(2)}}{\partial x_1}\right] \\
\rho \frac{\partial^2 u_3^1}{\partial t^2} &= C_{33} \frac{\partial^2 u_3^1}{\partial x_3^2} + C_{55} \frac{\partial^2 u_3^1}{\partial x_1^2} + (C_{55} + C_{13}) \frac{\partial^2 u_1^1}{\partial x_1 \partial x_3} - \frac{3}{b}\left[C_{44}\left(\frac{\partial u_2^0}{\partial x_3} + \frac{u_3^1}{b}\right) - C_{23} \frac{\partial u_2^{(2)}}{\partial x_3}\right]
\end{aligned}\right\} \qquad (11)$$

The first two equations describe the in-plane or extensional motion. Note that this motion depends on the thickness stretching u_2^1. The equation of motion for u_2^1, which is obtained from equation (8), is

$$\frac{2}{3} b\left[C_{66}\left(u_{2,11}^1 + \frac{3}{b} u_{1,1}^{(2)}\right) + C_{44}\left(u_{2,33}^1 + \frac{3}{b} u_{3,3}^{(2)}\right)\right]$$

$$- 2\left(C_{12} u_{1,1}^0 + C_{23} u_{3,3}^0 + \frac{C_{22}}{b} u_2^1\right) + q_2 = \frac{2}{3} \rho b \ddot{u}_2^1 \qquad (12)$$

The following approximation is made. We drop the higher order displacements in the displacement expansion, $u_1^{(2)}$, $u_3^{(2)}$, etc., in equation (6) and in equation (12). Next the terms containing second derivatives are dropped in equation (12), keeping only the low-frequency terms. This procedure leaves an explicit equation for u_2^1. A similar procedure is used on the equation for $u_2^{(2)}$ (which is not presented in full here). The simplified equations for u_2^1, $u_2^{(2)}$ are

$$\left.\begin{aligned}
q_2 - 2\left(C_{22} \frac{u_2^1}{b} + C_{12} \frac{\partial u_1^0}{\partial x_1} + C_{23} \frac{\partial u_3^0}{\partial x_3}\right) &= 0 \\
q_2 - 2\left(C_{22} \frac{3u_2^{(2)}}{b} + C_{12} \frac{\partial u_1^1}{\partial x_1} + C_{23} \frac{\partial u_3^1}{\partial x_3}\right) &= 0
\end{aligned}\right\} \qquad (13)$$

Using these equations, the terms u_2^1 and $u_2^{(2)}$ can be eliminated from equations (10) and (11). The resulting set of equations form the basis of our wave analysis:

$$\left.\begin{aligned}
\rho \frac{\partial^2 u_1^0}{\partial t^2} &= \left(C_{11} - \frac{C_{12}^2}{C_{22}}\right)\frac{\partial^2 u_1^0}{\partial x_1^2} + C_{55}\frac{\partial^2 u_1^0}{\partial x_3^2} + \left(C_{55} + C_{13} - \frac{C_{12}C_{13}}{C_{22}}\right)\frac{\partial^2 u_3^0}{\partial x_1\,\partial x_3} + \frac{C_{12}}{2C_{22}}\frac{\partial q_2}{\partial x_1} \\
\rho \frac{\partial^2 u_3^0}{\partial t^2} &= \left(C_{33} - \frac{C_{23}^2}{C_{22}}\right)\frac{\partial^2 u_3^0}{\partial x_3^2} + C_{55}\frac{\partial^2 u_3^0}{\partial x_1^2} + \left(C_{55} + C_{13} - \frac{C_{12}C_{23}}{C_{22}}\right)\frac{\partial^2 u_1^0}{\partial x_1\,\partial x_3} + \frac{C_{23}}{2C_{22}}\frac{\partial q_2}{\partial x_3}
\end{aligned}\right\} \quad (14)$$

$$\left.\begin{aligned}
\rho \frac{\partial^2 u_2^0}{\partial t^2} &= C_{66}\frac{\partial^2 u_2^0}{\partial x_1^2} + C_{44}\frac{\partial^2 u_2^0}{\partial x_3^2} + C_{66}\frac{1}{b}\frac{\partial u_1^1}{\partial x_1} + C_{44}\frac{1}{b}\frac{\partial u_3^1}{\partial x_3} + \frac{1}{2b}q_2 \\
\rho \frac{\partial^2 u_1^1}{\partial t^2} &= \left(C_{11} - \frac{C_{12}^2}{C_{22}}\right)\frac{\partial^2 u_1^1}{\partial x_1^2} + C_{55}\frac{\partial^2 u_1^1}{\partial x_3^2} + \left(C_{55} + C_{13} - \frac{C_{12}C_{23}}{C_{22}}\right)\frac{\partial^2 u_3^1}{\partial x_1\,\partial x_3} \\
&\quad - \frac{3}{b}C_{66}\left(\frac{\partial u_2^0}{\partial x_1} + \frac{u_1^1}{b}\right) + \frac{C_{12}}{2C_{22}}\frac{\partial q_2}{\partial x_1} \\
\rho \frac{\partial^2 u_3^1}{\partial t^2} &= \left(C_{33} - \frac{C_{23}^2}{C_{22}}\right)\frac{\partial^2 u_3^1}{\partial x_3^2} + C_{55}\frac{\partial^2 u_3^1}{\partial x_1^2} + \left(C_{55} + C_{13} - \frac{C_{12}C_{23}}{C_{22}}\right)\frac{\partial^2 u_1^1}{\partial x_1\,\partial x_3} \\
&\quad - \frac{3}{b}C_{44}\left(\frac{\partial u_2^0}{\partial x_3} + \frac{u_3^1}{b}\right) + \frac{C_{23}}{2C_{22}}\frac{\partial q_2}{\partial x_3}
\end{aligned}\right\} \quad (15)$$

It should be noted that in the procedure used by Mindlin (ref. 4) the coefficients C_{44} and C_{66} in equations (10) and (11) were replaced by k_3C_{44} and k_1C_{66}, respectively. The correction constants k_1 and k_3 were adjusted in order to match the thickness shear vibration mode (ref. 4). These terms will not enter the calculations presented herein.

WAVE PROPAGATION

Solutions to the propagation of plane waves in anisotropic plates are sought in the form

$$\underset{\sim}{u} = \underset{\sim}{f}(\underset{\sim}{n} \cdot \underset{\sim}{x} - vt) \tag{16}$$

where $\underset{\sim}{n}$ is a prescribed unit vector. If such a solution exists, $\underset{\sim}{u}$ can only change in the direction $\underset{\sim}{n}$, that is,

$$\nabla u_i = \frac{df_i(\varphi)}{d\varphi}\,\underset{\sim}{n}$$

or at a given time the displacement is constant on a plane normal to the vector $\underset{\sim}{n}$. When a solution of the form (16) exists, v is called the wave or phase speed.

Consider first the extensional motion which is governed by equations (14). Assume a solution in the form

$$\left.\begin{aligned} u_1^0 &= U_1 f(\underset{\sim}{n} \cdot \underset{\sim}{x} - vt) \\ u_3^0 &= U_3 f(\underset{\sim}{n} \cdot \underset{\sim}{x} - vt) \end{aligned}\right\} \tag{17}$$

Substituting these expressions into equations (14) reveals that U_1, U_3, and v must satisfy the following linear algebraic equations for a given $\underset{\sim}{n}$:

$$\begin{bmatrix} A_{11} & A_{12} \\ A_{21} & A_{22} \end{bmatrix} \begin{bmatrix} U_1 \\ U_3 \end{bmatrix} = v^2 \begin{bmatrix} U_1 \\ U_3 \end{bmatrix} \tag{18}$$

where

$$A_{11} = \left(C_{11} - \frac{C_{12}^2}{C_{22}}\right)\cos^2\varphi + C_{55}\sin^2\varphi$$

$$A_{22} = \left(C_{33} - \frac{C_{32}^2}{C_{22}}\right)\sin^2\varphi + C_{55}\cos^2\varphi$$

$$A_{12} = A_{21} = \left(C_{55} + C_{13} - \frac{C_{12}C_{23}}{C_{22}}\right)\sin\varphi\cos\varphi$$

$$\underset{\sim}{n} = (\cos\varphi,\ \sin\varphi)$$

Thus v^2 is a root of the equation

$$\Delta(\underset{\sim}{n},\ v^2) = \det\left(A_{ij} - \rho v^2 \delta_{ij}\right) = 0 \tag{19}$$

where δ_{ij} is the Kronecker delta ($\delta_{12} = \delta_{21} = 0$ and $\delta_{11} = \delta_{22} = 1$). The physically possible elastic constants $C_{\alpha\beta}$ will guarantee that A_{ij} is positive definite. This guarantees two positive real roots v_1^2 and v_2^2 for a given wave normal $\underset{\sim}{n}$.

The ratio U_1/U_3 will be determined by substituting each root v^2 into the equations (19). Since $A_{ij} = A_{ji}$, the displacement vectors corresponding to the roots v_1^2 and v_2^2 will be orthogonal to each other. If the displacement direction, determined by U_1/U_3, is parallel to $\underset{\sim}{n}$, the wave is called longitudinal; if the displacement corresponding to U_1/U_3 is normal to $\underset{\sim}{n}$, the wave is called transverse. For isotropic materials it is known that the wave motion is longitudinal for the larger root, and transverse for the smaller root. For anisotropic materials, the velocity v depends on $\underset{\sim}{n}$, and the motion is neither longitudinal nor transverse except for certain symmetry directions.

Consider next the bending equations (15). One can show that the only plane wave solutions of the form (16) that satisfy equations (15) are harmonic functions, that is,

$$\begin{bmatrix} u_1^1 \\ u_3^1 \\ u_2^0 \end{bmatrix} = \begin{bmatrix} b\psi_1 \\ b\psi_3 \\ U_2 \end{bmatrix} e^{ik(\underset{\sim}{n}\cdot\underset{\sim}{x}-vt)} \tag{20}$$

The product $\omega = kv$ is called the frequency; k is called the wave number or inverse wavelength. For bending motion, the phase velocity v depends on the frequency ω as well as the wave normal $\underset{\sim}{n}$. Mindlin (ref. 4) has examined the dependence of v on ω for various material anisotropies.

Thus the behavior of the bending motion at the wave fronts cannot be determined in the same manner as was the extensional motion. Instead of finding a valid solution for the whole impact disturbed area of the plate, we consider the motion at the wave front only. Across this front, one imagines that certain quantities have discontinuities. The displacement and the stress are assumed to be continuous across the wave front but allow discontinuities in the second derivatives of U. Such waves are called acceleration waves (ref. 6, chapt. 5).

Let $[\psi]$ denote the jump in the function $\psi(x_1, x_3)$ across the wave front. Then by assumption we have (where i, j = 1 or 3)

$$\left[U^0_{2,1}\right] = \left[U^0_{2,3}\right] = 0$$

$$\left[U^1_{1,1}\right] = \left[U^1_{1,3}\right] = 0$$

$$\left[U^1_{3,1}\right] = \left[U^1_{3,3}\right] = 0$$

The second derivatives are assumed to exist on both sides of the wave front; thus, we can write the equations of motion for bending (eq. (15)) on both sides of the wave front and subtract one from the other, from which results

$$\rho\left[\frac{\partial u_2^0}{\partial t^2}\right] = C_{66}\left[\frac{\partial^2 u_2^0}{\partial x_1^2}\right] + C_{44}\left[\frac{\partial^2 u_2^0}{\partial x_3^2}\right] \tag{21}$$

$$\rho\left[\frac{\partial^2 u_1^1}{\partial t^2}\right] = \left(C_{11} - \frac{C_{12}^2}{C_{22}}\right)\left[\frac{\partial^2 u_1^1}{\partial x_1^2}\right] + C_{55}\left[\frac{\partial^2 u_1^1}{\partial x_3^2}\right] + \left(C_{55} + C_{13} - \frac{C_{12}C_{23}}{C_{22}}\right)\left[\frac{\partial^2 u_3^1}{\partial x_1\, \partial x_3}\right]$$

$$\rho\left[\frac{\partial^2 u_3^1}{\partial t^2}\right] = \left(C_{33} - \frac{C_{23}^2}{C_{22}}\right)\left[\frac{\partial^2 u_3^1}{\partial x_3^2}\right] + C_{55}\left[\frac{\partial^2 u_3^1}{\partial x_3^2}\right] + \left(C_{55} + C_{13} - \frac{C_{12}C_{23}}{C_{23}}\right)\left[\frac{\partial^2 u_1^1}{\partial x_1\, \partial x_3}\right]$$

The jump in acceleration, however, is not independent of the jump in the strain gradient. It can be shown that for a plane wave front with unit normal $\underset{\sim}{n}$, the following relations hold:

$$\left[\frac{\partial^2 \psi}{\partial x_i\, \partial x_j}\right] = \frac{n_i n_j}{v^2}\left[\frac{\partial^2 \psi}{\partial t^2}\right] \tag{22}$$

The quantity v is called the wave front speed in the normal direction. This relation can then be used in the preceding equations to obtain linear algebraic relati between the discontinuities in acceleration across the front:

$$\rho v^2 = C_{66}\cos^2\varphi + C_{44}\sin^2\varphi$$

$$\begin{bmatrix} A_{11} & A_{12} \\ A_{21} & A_{22} \end{bmatrix}\begin{bmatrix} a_1 \\ a_2 \end{bmatrix} = v^2\begin{bmatrix} a_1 \\ a_2 \end{bmatrix} \tag{23}$$

where

$$a_1 = \left[\frac{\partial^2 u_1^1}{\partial t^2}\right] \qquad a_2 = \left[\frac{\partial^2 u_3^1}{\partial t^2}\right]$$

$$n_1 = \cos\varphi \qquad n_3 = \sin\varphi$$

and A_{ij} are exactly the same constants that occur in equation (18).

Thus the wave fronts associated with a jump in the bending accelerations $\partial^2 u_1^1 / \partial t^2$

and $\partial^2 u_3^1/\partial t^2$ travel at the same speeds as the wave front associated with the extensional motion. There is another wave front corresponding to a jump in the quantity $\partial^2 u_2^0/\partial t^2$. For the case of a composite with symmetric ply orientation about the midplane,

$$C_{66} = C_{44}$$

The bending wave associated with the jump $\partial u_2^0/\partial t^2$ is thus isotropic.

If both extensional and bending motions are generated simultaneously by impact, the two extensional and two bending wave fronts will travel with the same wave speeds.

The analysis presented here is not unique. The same results can be obtained if one considers the equations of motion (14) and (15) from the method of characteristics (ref. 6).

The velocity surfaces $v = v(\underset{\sim}{n})$ have been computed for various fiber composites and ply configurations. These results are discussed in a later section.

WAVE SURFACES

In the preceding section we outlined how plane waves would travel in an anisotropic plate. The phase velocity of two of the modes was found to depend on the orientation of the wave normal to the symmetry axes of the plate. This angle we called φ. Suppose, then, that a plate receives a transverse impact at the origin of a coordinate system (r, θ). The disturbance can be thought of as a superposition of plane waves. To an observer at position (r_0, θ_0), the first signal to arrive may not be that corresponding to the wave normal $\varphi = \theta_0$. If t is the arrival time, the first plane wave $\underset{\sim}{n}(\varphi)$ to arrive at the point $\underset{\sim}{r}$ must satisfy (see fig. 1)

$$\underset{\sim}{r} \cdot \underset{\sim}{n}(\varphi) = v(\varphi)t$$

For a given time (say $t = 1$) the wave surface is defined as the locus of points $\underset{\sim}{r}$ which satisfy (unpublished notes by Yih-Hsing Pao)

$$\underset{\sim}{r} \cdot \underset{\sim}{s} = 1 \tag{24}$$

where

$$\underset{\sim}{s} = \frac{\underset{\sim}{n}(\varphi)}{v(\varphi)}$$

The vector $\underset{\sim}{s}$ is called the slowness vector, and the surface $1/v(\varphi)$ is called the slowness surface. (A good discussion of the properties of velocity, slowness, and wave surfaces may be found in ref. 2.)

Instead of finding the first arrival wave $\underset{\sim}{n}(\varphi)$ for a given $\underset{\sim}{r}$, we determine $\underset{\sim}{r}$ for a given plane wave $\underset{\sim}{n}$ such that equation (24) is satisfied, with $\underset{\sim}{r}$ fixed. Then, the equation $\underset{\sim}{s} \cdot \underset{\sim}{r} = 1$ represents a line in the slowness plane and $\underset{\sim}{r}$ the normal to that line. However, not all $\underset{\sim}{s}$ are admissible; $\underset{\sim}{s}$ has to be on the slowness surface. Thus, the line $\underset{\sim}{s} \cdot \underset{\sim}{r} = 1$ is tangent to the slowness surface and $\underset{\sim}{r}$ is the normal vector to that surface. Suppose the slowness surface is given by the equation

$$g(\underset{\sim}{s}) = 0 \tag{25}$$

Then

$$\underset{\sim}{r} = \lambda \underset{\sim}{N} \tag{26}$$

where

$$\underset{\sim}{N} = \nabla g(\underset{\sim}{s})$$

Substituting this expression for $\underset{\sim}{r}$ into equation (24) yields

$$\lambda = \frac{v}{\underset{\sim}{n} \cdot \nabla g(\underset{\sim}{s})}$$

and

$$\underset{\sim}{r} = \frac{v \nabla g(\underset{\sim}{s})}{\underset{\sim}{n} \cdot \nabla g(\underset{\sim}{s})} \tag{27}$$

In our case v and hence $1/v$ are roots of a quadratic equation (19), that is,

$$v^4 - a_1(\varphi)v^2 + a_2(\varphi) = 0$$

or

$$g(\underset{\sim}{s}) = a_2(\varphi)s^4 - a_1(\varphi)s^2 + 1 = 0$$

Thus,

$$\nabla g(\underset{\sim}{s}) = \frac{\partial g}{\partial s}\,\underset{\sim}{e}_s + \frac{1}{s}\,\frac{\partial g}{\partial \varphi}\,\underset{\sim}{e}_\varphi$$

$$\frac{\partial g}{\partial s} = 2s\left(2s^2 a_2 - a_1\right)$$

$$\frac{1}{s}\,\frac{\partial g}{\partial \varphi} = s\left(s^2\,\frac{\partial a_2}{\partial \varphi} - \frac{\partial a_1}{\partial \varphi}\right)$$

For each root v there is a wave surface. It can be shown (ref. 3) that the outer surface, which is associated with the fastest velocity, is strictly convex. However, the slower velocity surface can result in a wave surface with cusp points.

The locus of $\underset{\sim}{r}(\varphi)$ has been computed for various fiber composite systems and fiber layup angles. The results are shown in figure 2 and are discussed in the following section.

DISCUSSION OF NUMERICAL RESULTS

Velocity, slowness, and wave surfaces were calculated for various anisotropies corresponding to various fiber composite plates using a digital computer. The three fiber-matrix systems examined were graphite-epoxy, boron-aluminum, and glass-epoxy. The equivalent elastic constants for these fiber-matrix systems at various layup angles (fig. 1) were obtained by Chamis (ref. 7). These constants, which are listed in tables I to III, are based on a statistical analysis of an eight-ply plate using the known properties of each fiber-matrix ply.

The velocity and wave surfaces for a boron-aluminum composite are shown in figure 2. The ratio of moduli $C_{11}/C_{33} = 1.2$. This results in different wave speeds in the two principal directions. However, the shear velocity is almost isotropic. The wave surfaces (fig. 2(b)), while showing the effects of anisotropy, exhibit no peculiarities.

The graphite-epoxy system contrasts with the boron-aluminum system because of its high stiffness ratio; $C_{11}/C_{33} = 24$ (zero layup angle). The velocity surfaces for layup angles of $\pm 0^\circ$, $\pm 15^\circ$, $\pm 30^\circ$, and $\pm 45^\circ$ are shown in figure 3. It is interesting to note that, as the fiber orientation approaches $\pm 45^\circ$, the anisotropy in the larger wave velocity (quasi-longitudinal wave) diminishes, but that of the smaller root (quasi-shear wave) increases.

The resulting wave surfaces for graphite-epoxy are shown in figure 4. (The slow-

TABLE I. - STRESS-STRAIN COEFFICIENTS FOR 55 PERCENT BORON

FIBER-ALUMINUM MATRIX COMPOSITE

[Material density, 2.65 g/cm^3; all constants to be multiplied by 10^6 psi; data obtained from ref. 7.]

0° Layup					
42.80	11.44	11.44	0	0	0
	34.47	14.92	0	0	0
		34.47	0	0	0
			9.775	0	0
				13.18	0
					9.775

15° Layup					
42.14	11.67	11.54	0	0	0
	34.47	14.68	0	0	0
		34.92	0	0	0
			9.775	0	0
				13.29	0
					9.775

$\pm30^\circ$ Layup					
40.40	12.31	11.75	0	0	0
	34.47	14.05	0	0	0
		36.24	0	0	0
			9.775	0	0
				13.49	0
					9.775

$\pm45^\circ$ Layup					
38.22	13.18	11.85	0	0	0
	34.47	13.18	0	0	0
		38.22	0	0	0
			9.775	0	0
				13.60	0
					9.775

TABLE II. - STRESS-STRAIN COEFFICIENTS FOR 55 PERCENT GRAPHITE

FIBER-EPOXY MATRIX COMPOSITE

[Material density, 1.44 g/cm^3; all constants to be multiplied by 10^6 psi; data obtained from ref. 7.]

0° Layup					
27.95	0.3957	0.3957	0	0	0
	1.170	0.4601	0	0	0
		1.170	0	0	0
			0.3552	0	0
				0.7197	0
					0.3552

$\pm15^\circ$ Layup					
24.56	0.4000	1.986	0	0	0
	1.170	0.4558	0	0	0
		1.374	0	0	0
			0.3552	0	0
				2.310	0
					0.3552

$\pm30^\circ$ Layup					
16.48	0.4118	5.167	0	0	0
	1.170	0.4400	0	0	0
		3.093	0	0	0
			0.3552	0	0
				5.491	0
					0.3552

$\pm45^\circ$ Layup					
8.197	0.4279	6.758	0	0	0
	1.170	0.4279	0	0	0
		8.197	0	0	0
			0.3552	0	0
				7.082	0
					0.3552

TABLE III. - STRESS-STRAIN COEFFICIENTS FOR 55 PERCENT GLASS FIBER-EPOXY MATRIX COMPOSITE

[Material density, 1.92 g/cm^3; all constants to be multiplied by 10^6 psi; data obtained from ref. 7.]

0° Layup						$\pm 15^\circ$ Layup					
7.500	0.9097	0.9097	0	0	0	6.890	0.9321	1.178	0	0	0
	2.395	1.244	0	0	0		2.395	1.222	0	0	0
		2.395	0	0	0			2.468	0	0	0
			0.5753	0	0				0.5753	0	0
				0.9457	0					1.214	0
					0.5753						0.5753
$\pm 30^\circ$ Layup						$\pm 45^\circ$ Layup					
5.419	0.9933	1.715	0	0	0	3.874	1.077	1.983	0	0	0
	2.395	1.161	0	0	0		2.395	1.077	0	0	0
		2.866	0	0	0			3.874	0	0	0
			0.5753	0	0				0.5753	0	0
				1.751	0					2.019	0
					0.5753						0.5753

ness surface is shown in fig. 5.) In contrast to the boron-aluminum system, the quasi-shear surfaces show peculiar cusps and nonconvexity. This behavior is also characteristic of crystal systems such as zinc. Unlike the natural crystals, we can change the wave properties, without changing the material constituents, by varying the fiber layup angle. It becomes clear that, as the anisotropy in the quasi-longitudinal wave is reduced (i.e., $\varphi \rightarrow 45^\circ$), the cusped behavior of the quasi-shear waves increases. This is due to the previously mentioned increase in shear wave anisotropy as $\varphi \rightarrow 45^\circ$ (fig. 3).

Another peculiar property of wave propagation in this composite system can be noted by examination of the $\pm 45^\circ$ fiber layup case (fig. 4(d)). On the outer wave surface, the angle of the wave normal of the first arrival plane wave is listed. One can see that the distribution of plane wave normals is heavily concentrated at positions on the wave surface close to the fiber directions. This might imply a focusing of waves along the fiber directions. For the other fiber orientations, the distribution of wave normals is also concentrated at those points on the wave surface close to the fiber directions but not as densely as in the $\pm 45^\circ$ layup case. The implications of this wave focusing along the fiber direction will not be made completely clear until the stress and displacement fields are found.

Similar results for the glass fiber-epoxy composite system are presented in figures 6 and 7. The ratio of stiffnesses for this case is $C_{11}/C_{33} = 3.1$ (zero layup angle). The wave surfaces for this system show features similar to the graphite-epoxy case. Note, however, that for a layup angle of $\pm 15^{\circ}$, the quasi-shear wave velocity is almost isotropic (fig. 6). This results in a wave surface (fig. 7(c)) with no cusped behavior. Although not as marked as the graphite-epoxy case, this system also exhibits a wave normal focusing along the fiber directions.

Lewis Research Center,
National Aeronautics and Space Administration,
Cleveland, Ohio, March 5, 1971,
129-03.

REFERENCES

1. Lekhnitskii, S. G. (P. Fern, trans.): Theory of Elasticity of an Anisotropic Elastic Body. Holden-Day Publ., 1963.

2. Kraut, Edgar A.: Advances in the Theory of Anisotropic Elastic Wave Propagation. Rev. Geophysics, vol. 1, no. 3, Aug. 1963, pp. 401-448.

3. Musgrave, M. J. P.: Elastic Waves in Anisotropic Media. Progress in Solid Mechanics. Vol. 2. I. N. Sneddon and R. Hill, eds., Interscience Publ., 1961, pp. 64-85.

4. Mindlin, R. D.: High Frequency Vibrations of Crystal Plates. Quart. Appl. Math., vol. 19, no. 1, Apr. 1961, pp. 51-61.

5. Mindlin, R. D.; and Medick, M. A.: Extensional Vibrations of Elastic Plates. J. Appl. Mech., vol. 26, no. 4, Dec. 1959, pp. 561-569.

6. Courant, Richard; and Hilbert, David: Methods of Mathematical Physics. Interscience Publ., 1962.

7. Chamis, C. C.: Computer Code for the Analysis of Multilayered Fiber Composites - Users Manual. NASA TN D-7013, 1971.

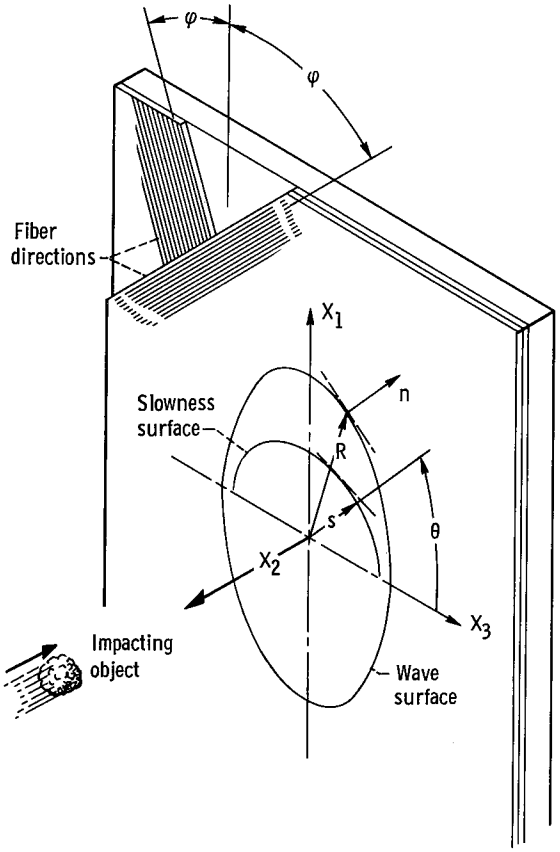

Figure 1. - Diagram notation and sign convention for plate element.

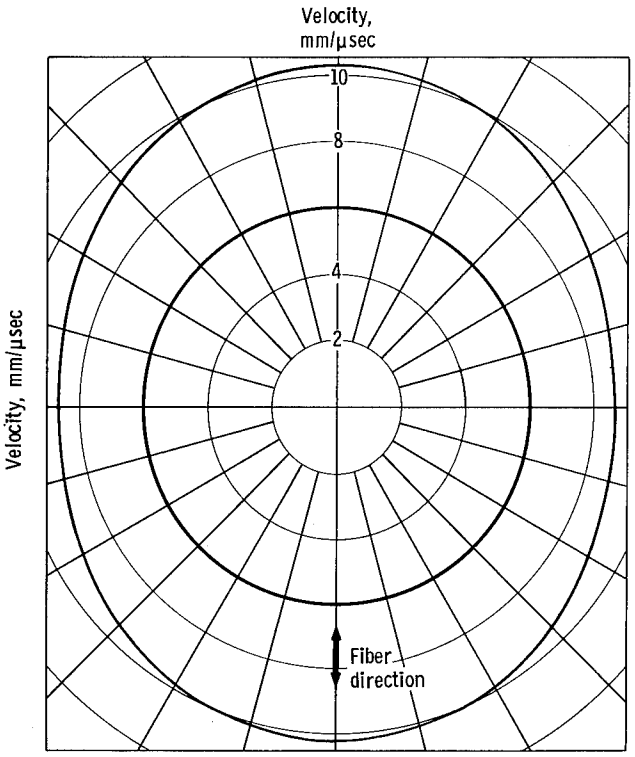

(a) Velocity surfaces.

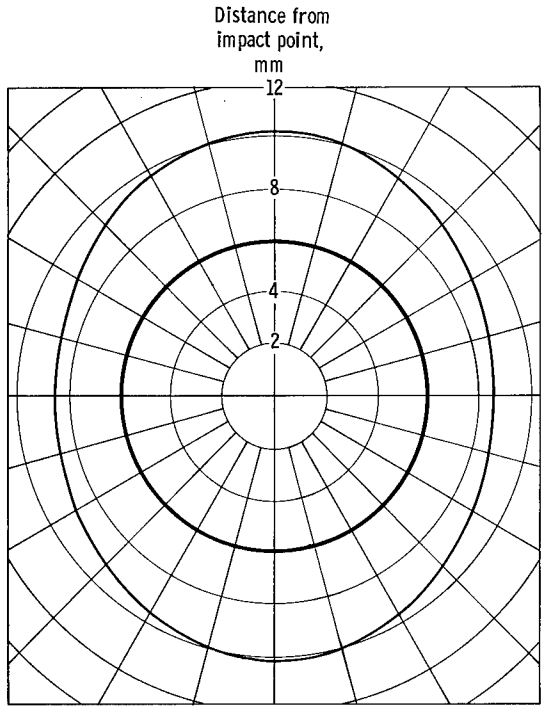

(b) Wave surfaces at 1 microsecond after impact.

Figure 2. - Velocity and wave surfaces for 55 percent boron fiber - aluminum matrix plates. Fiber layup angle, 0^{0}.

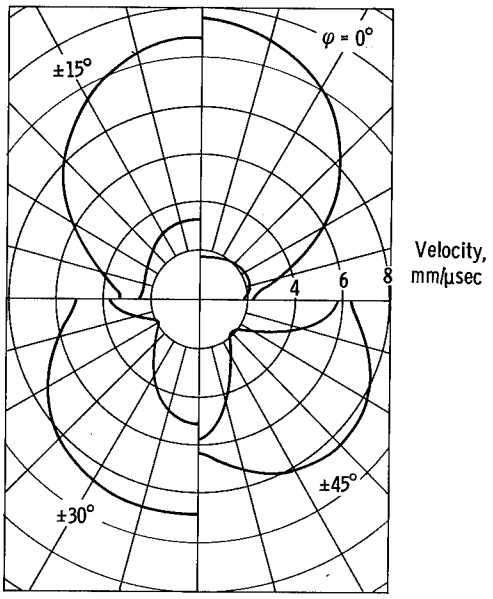

Figure 3. - Velocity surfaces for 55 percent graphite fiber-epoxy matrix plates at various layup angles.

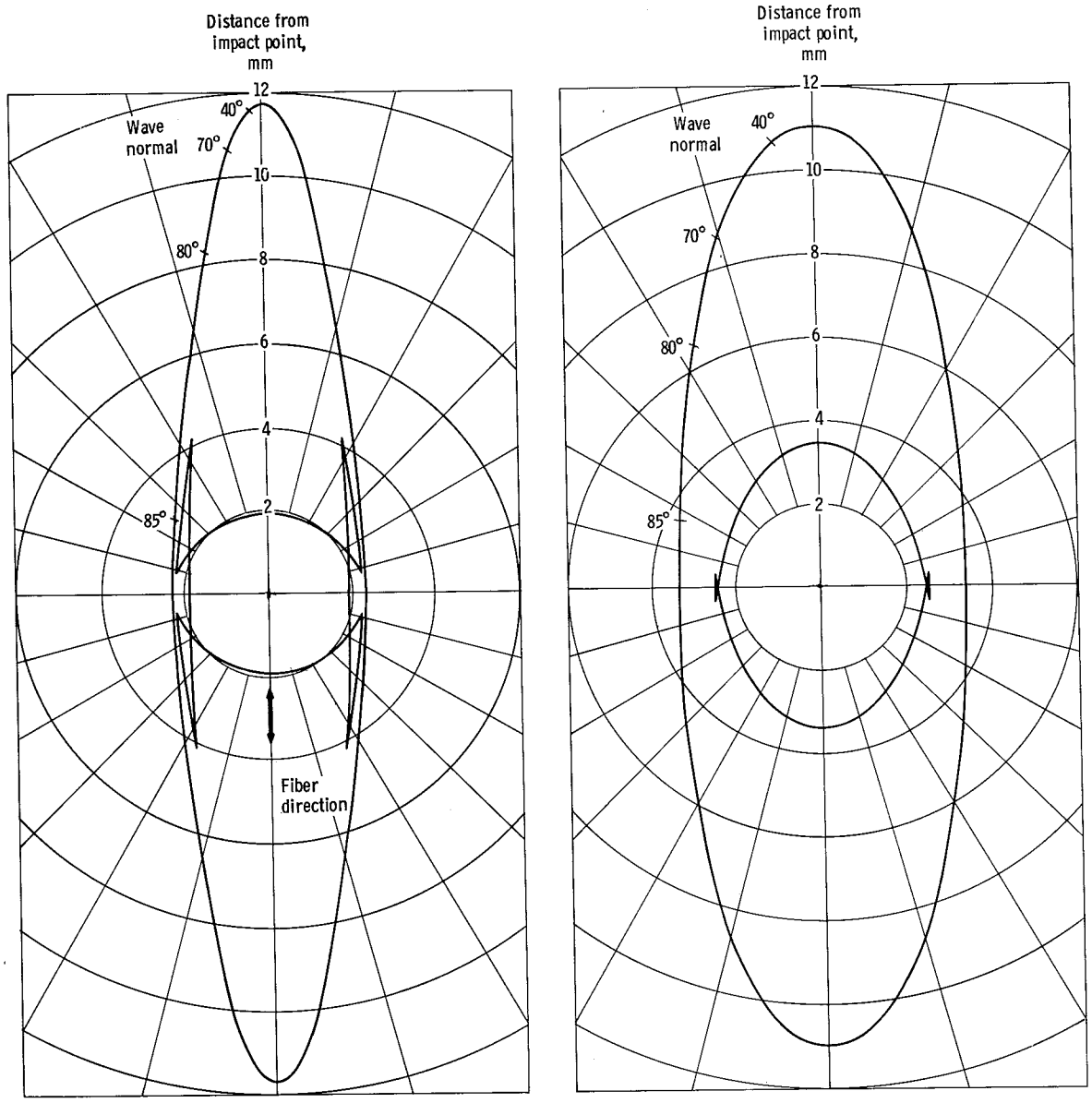

(a) Fiber layup angle, 0°.

(b) Fiber layup angle, ±15°.

Figure 4. - Wave surfaces at 1 microsecond after impact for 55 percent graphite fiber - epoxy matrix plates.

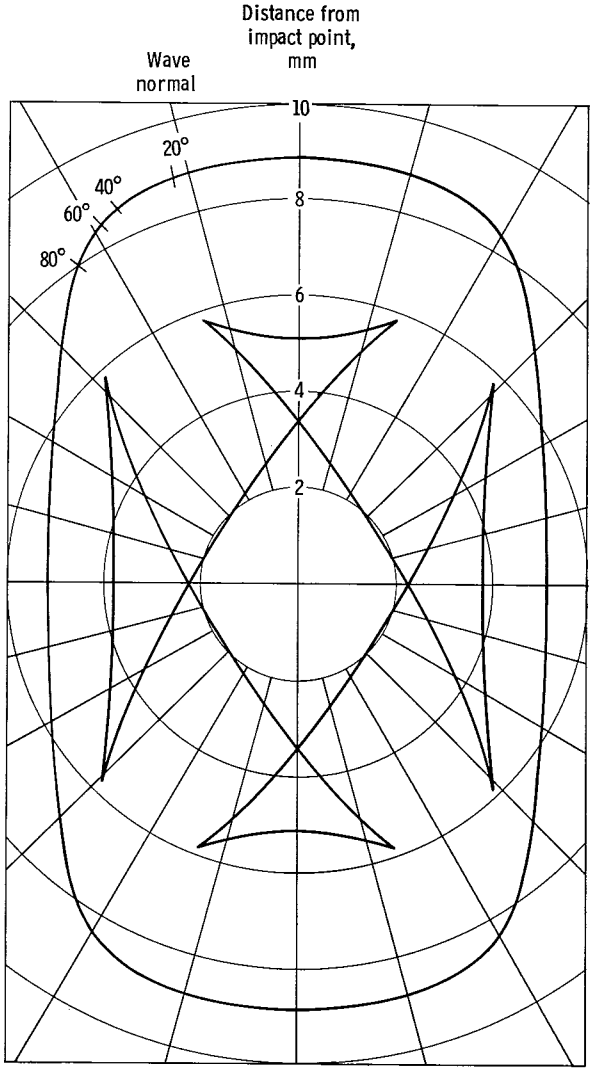

(c) Fiber layup angle, ±30°.

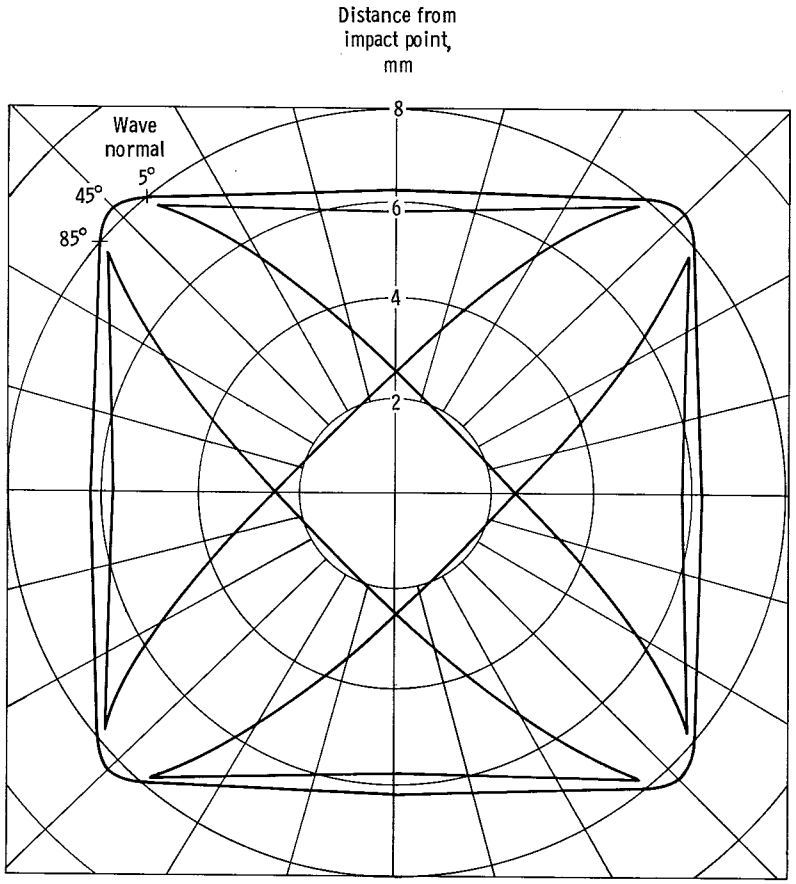

(d) Fiber layup angle, ±45°.

Figure 4. - Concluded.

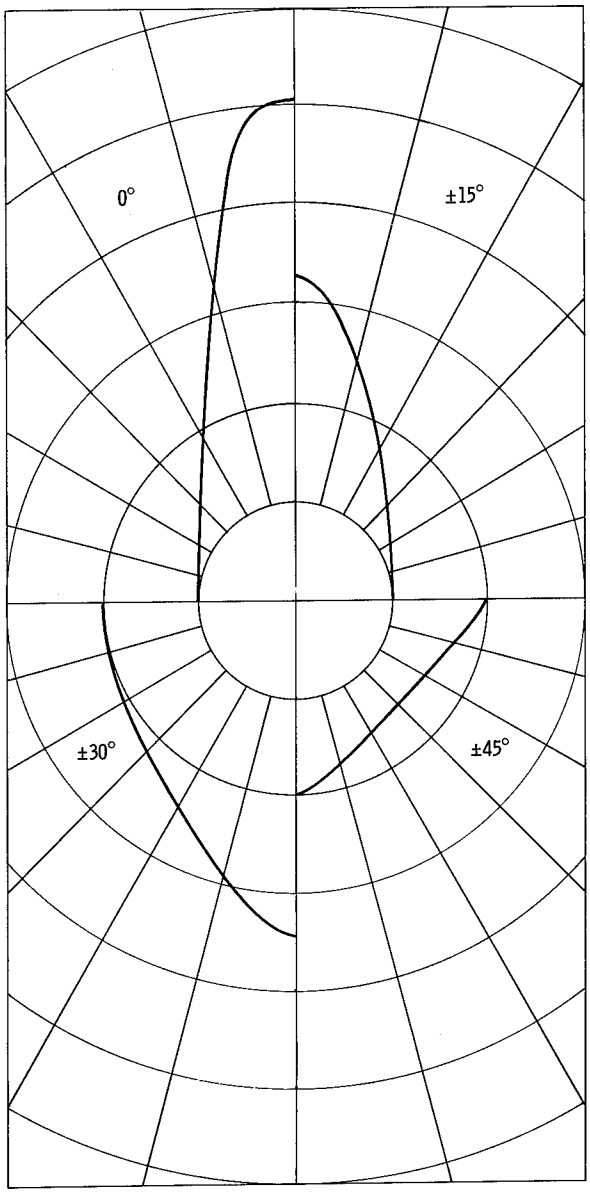

Figure 5. - Normalized slowness surfaces for 55 percent graphite fiber - epoxy matrix plates at various fiber layup angles.

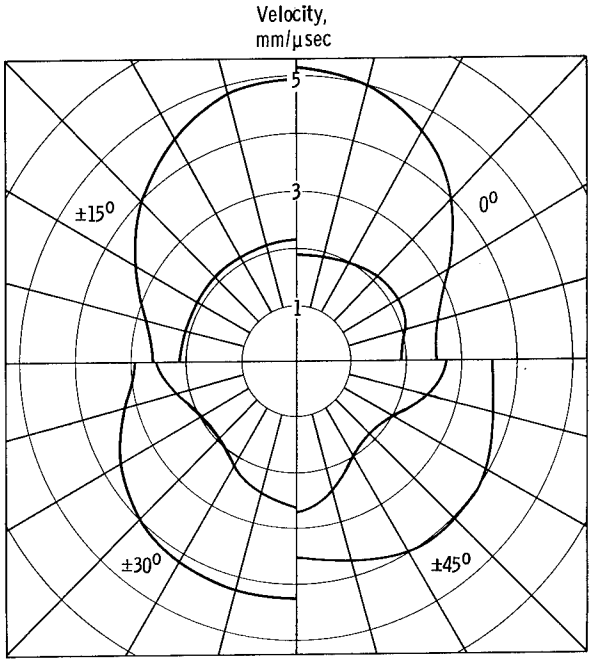

Figure 6. - Velocity surfaces for 55 percent glass fiber - epoxy matrix plates for various fiber layup angles.

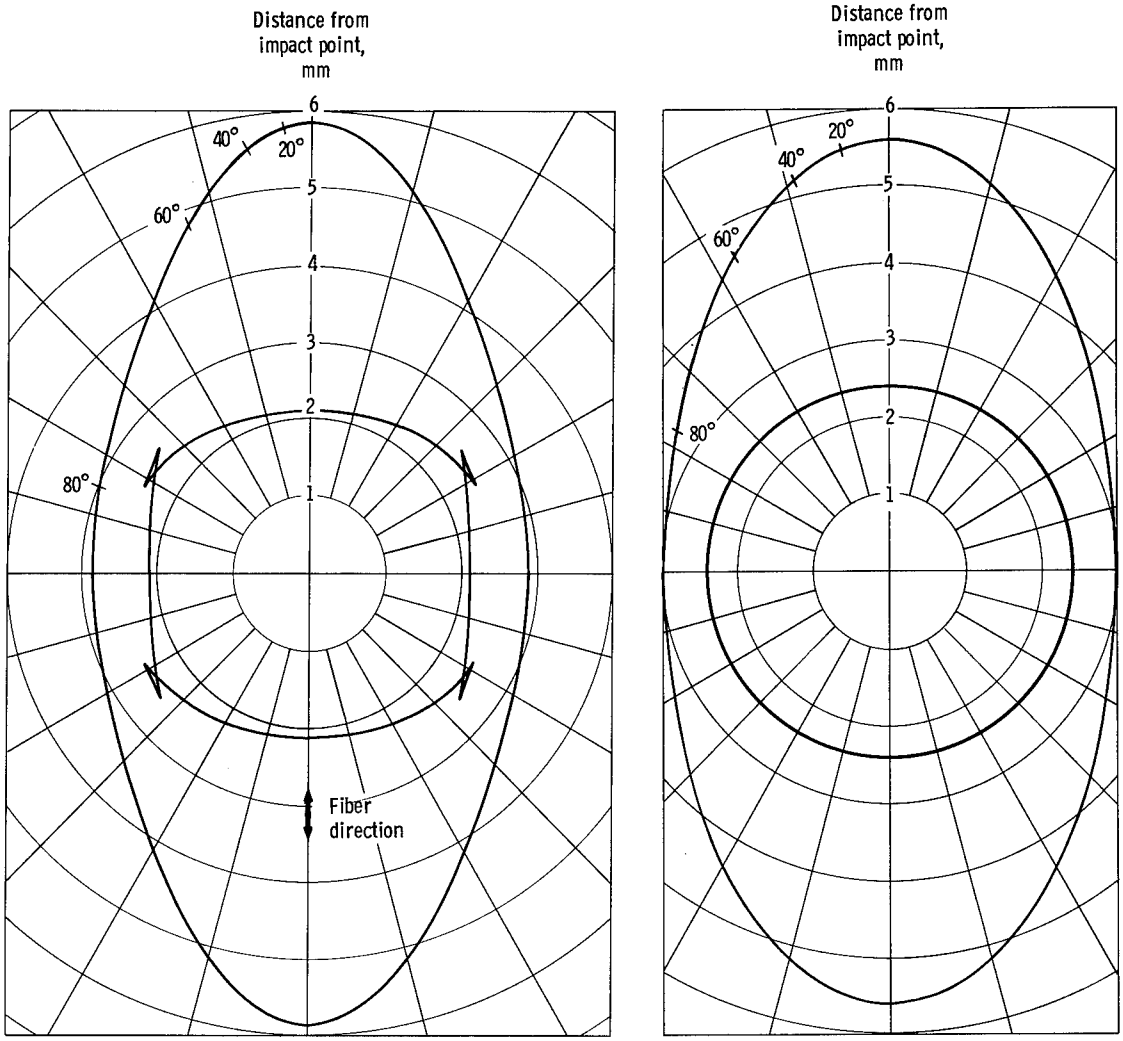

(a) Fiber layup angle, 0°.

(b) Fiber layup angle, ±15°.

Figure 7. - Wave surfaces at 1.15 microseconds after impact for 55 percent glass fiber - epoxy matrix plates.

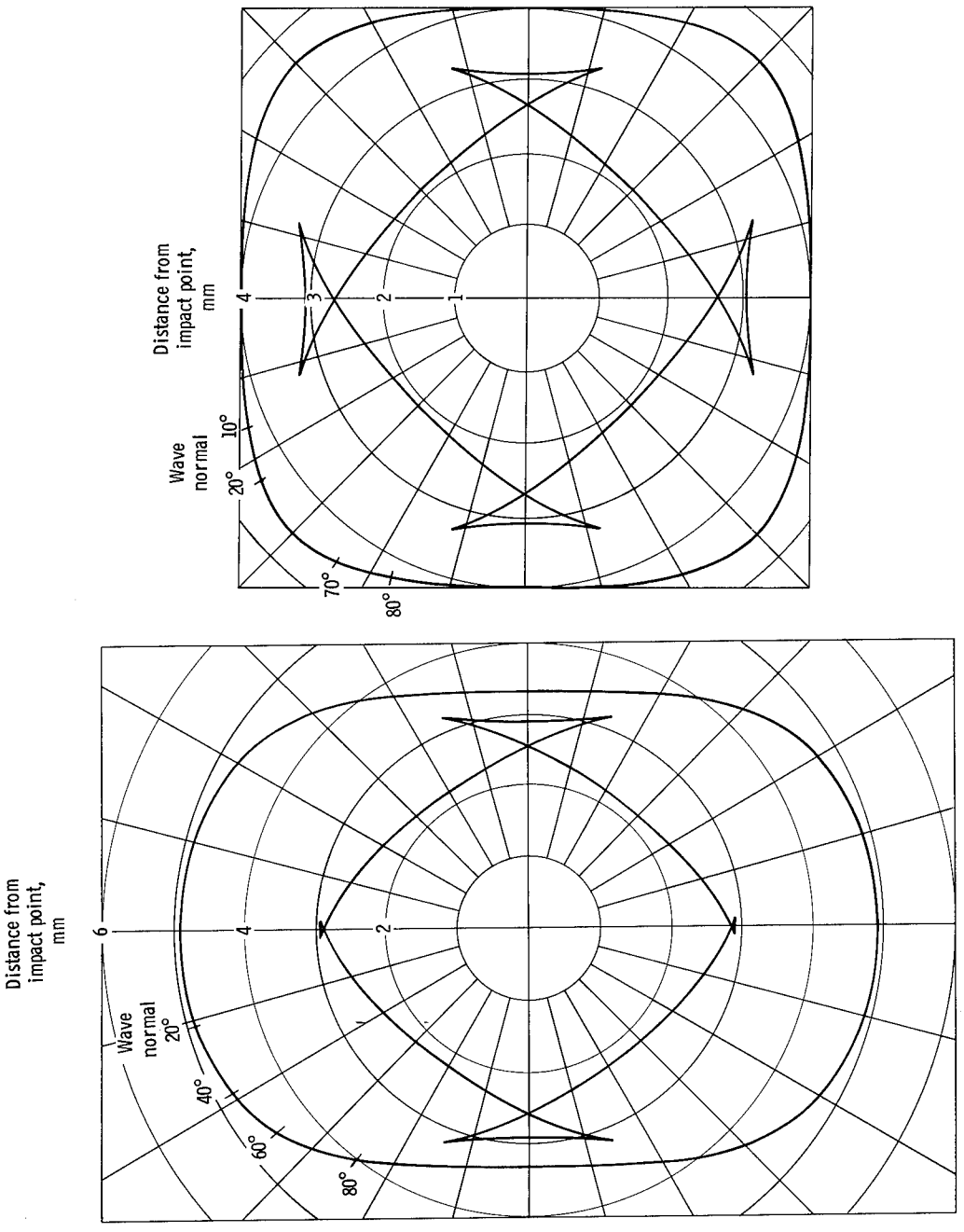

(c) Fiber layup angle, ±30°.

(d) Fiber layup angle, ±45°.

Figure 7. - Concluded.

NASA-Langley, 1971 —— 32 E-6150

"The aeronautical and space activities of the United States shall be conducted so as to contribute . . . to the expansion of human knowledge of phenomena in the atmosphere and space. The Administration shall provide for the widest practicable and appropriate dissemination of information concerning its activities and the results thereof."

—NATIONAL AERONAUTICS AND SPACE ACT OF 1958

NASA SCIENTIFIC AND TECHNICAL PUBLICATIONS

TECHNICAL REPORTS: Scientific and technical information considered important, complete, and a lasting contribution to existing knowledge.

TECHNICAL NOTES: Information less broad in scope but nevertheless of importance as a contribution to existing knowledge.

TECHNICAL MEMORANDUMS: Information receiving limited distribution because of preliminary data, security classification, or other reasons.

CONTRACTOR REPORTS: Scientific and technical information generated under a NASA contract or grant and considered an important contribution to existing knowledge.

TECHNICAL TRANSLATIONS: Information published in a foreign language considered to merit NASA distribution in English.

SPECIAL PUBLICATIONS: Information derived from or of value to NASA activities. Publications include conference proceedings, monographs, data compilations, handbooks, sourcebooks, and special bibliographies.

TECHNOLOGY UTILIZATION PUBLICATIONS: Information on technology used by NASA that may be of particular interest in commercial and other non-aerospace applications. Publications include Tech Briefs, Technology Utilization Reports and Technology Surveys.

Details on the availability of these publications may be obtained from:

SCIENTIFIC AND TECHNICAL INFORMATION OFFICE

NATIONAL AERONAUTICS AND SPACE ADMINISTRATION

Washington, D.C. 20546